Havel, T. F., & Wuthrich, K. (1985) *J. Mol. Biol. 182*, 281-294.
Holak, T. A., & Prestegard, J. H. (1986) *Biochemistry 26*, 5766-5774.
Holak, T. A., Prestegard, J. H., & Forman, J. D. (1987a) *Biochemistry 26*, 4652-4660.
Holak, T. A., Scarsdale, J. N., & Prestegard, J. H. (1987b) *J. Magn. Reson. 74*, 546-549.
Holak, T. A., Nilges, M., Prestegard, J. H., Gronenborn, A. M., & Clore, G. M. (1988) *Eur. J. Biochem.* (in press).
Jones, P. J., Cioffi, E. A., & Prestegard, J. H. (1987) *J. Biol. Chem. 262*, 8963-8965.
Kaptein, R., Zuiderweg, E. R. P., Scheck, R. M., Boelens, R., & van Gunsteren, W. F. (1985) *J. Mol. Biol. 196*, 611-639.
Mackay, A. L. (1983) *Acta Crystallogr., Sect. A: Found. Crystallogr. A40*, 165.
Macura, S., & Ernst, R. R. (1980) *Mol. Phys. 41*, 95-117.
Mayo, K. H., Tyrell, P. M., & Prestegard, J. H. (1983) *Biochemistry 22*, 4485-4493.
McRee, D. E., Richardson, J. S., & Richardson, D. C. (1985) *J. Mol. Biol. 182*, 467-468.
Ohlrogge, J. B. (1987) in *The Biochemistry of Plants*, Vol. 9, pp 137-157, Academic, New York.
Olejniczak, E. T., Dobson, C. M., Karplus, M., & Levy, R. M. (1984) *J. Am. Chem. Soc. 106*, 1923-1930.
Otting, G., Widmer, H., Wagner, G., & Wuthrich, K. (1986) *J. Magn. Reson. 66*, 187-193.
Scarsdale, J. N., Yu, R. K., & Prestegard, J. H. (1986) *J. Am. Chem. Soc. 108*, 6778-6784.
Scarsdale, J. N., Ram, P., Yu, R. K., & Prestegard, J. H. (1988) *J. Comput. Chem. 9*, 133-147.
Simoni, R. D., Criddle, R. S., & Stumpf, P. K. (1967) *J. Biol. Chem. 242*, 573-581.
Singh, V. C., & Kollman, P. A. (1984) *J. Comput. Chem. 5*, 129-145.
Spencer, A. K., Greenspan, A. D., & Cronan, J. E., Jr. (1978) *J. Biol. Chem. 253*, 5922-5926.
States, D. J., Habercorn, R. A., & Ruben, D. J. (1982) *J. Magn. Reson. 48*, 286-292.
Thompson, G. A., Jr. (1980) *The Regulation of Membrane Lipid Metabolism*, pp 19-43, CRC, Boca Raton, FL.
Wagner, G., Braun, W., Havel, T. F., Schaumann, T., Go, N., & Wuthrich, K. (1987) *J. Mol. Biol. 196*, 611-639.
Weiner, P. K., & Kollman, P. A. (1981) *J. Comput. Chem. 2*, 287-303.
Williamson, M. P., Havel, T. F., & Wuthrich, K. (1985) *J. Mol. Biol. 182*, 295-315.
Wuthrich, K. (1986) *NMR of Proteins and Nucleic Acids*, Wiley, New York.
Wuthrich, K., Billeter, M., & Braun, W. (1983) *J. Mol. Biol. 169*, 949-961.

Circular Dichroism and Potentiometry of FAD, Heme and Mo-Pterin Prosthetic Groups of Assimilatory Nitrate Reductase†

Christopher J. Kay,* Michael J. Barber, and Larry P. Solomonson
Department of Biochemistry, College of Medicine, University of South Florida, Tampa, Florida 33612
Received December 3, 1987; Revised Manuscript Received March 14, 1988

ABSTRACT: Oxidation-reduction midpoint potentials for flavin, heme, and molybdenum-pterin prosthetic groups of assimilatory nitrate reductase (NR) from *Chlorella vulgaris* were measured at room temperature by using CD and EPR potentiometry. The CD changes accompanying reduction of each prosthetic group were determined by using enzyme fragments containing either FAD or heme and molybdenum prosthetic groups, obtained by limited proteolysis, and by poising the enzyme at various redox potentials in the presence of dye mediators. Limited proteolysis did not appear to alter the environment of the prosthetic groups, as judged by their CD spectra. Also, CD potentiometric titration of FAD in intact NR (E_m' = −272 mV, n = 2) gave a similar value (E_m' = −286 mV) to the FAD of the flavin-containing proteolytic domain, determined by visible spectroscopy. Less than 1% of the flavin semiquinone was detected by EPR spectroscopy, indicating that E_m' (FAD/FAD$^{\bullet-}$) may be more than 200 mV lower than E_m' (FAD$^{\bullet-}$/FADH$^-$). Reduction of heme resulted in splitting of both Soret and α CD bands into couplets. The heme E_m' was −162 mV (n = 1) determined by both CD and visible spectroscopy. Reduction of Mo-pterin was followed by CD at 333 nm, and Mo(V) was monitored by room temperature EPR spectroscopy. Most of the change in the Mo-pterin CD spectrum was due to the Mo(VI)/Mo(V) transition. The E_m' values determined for Mo(VI)/Mo(V) were +26 mV by CD and +16 mV by EPR, whereas Mo(V)/Mo(IV) values were −40 mV by CD and −26 mV by EPR. In contrast, freezing samples to 100 K resulted in significant redistribution of electrons, particularly affecting the measured Mo(VI)/Mo(V) couple (−34 mV).

Assimilatory nitrate reductase (NR)[1] from *Chlorella vulgaris* catalyzes the initial and rate-limiting step, the NADH-dependent reduction of nitrate to nitrite, in the process of nitrate assimilation (Guerro et al., 1981). The enzyme exists as a homotetramer, with each subunit (M_r 96 000) containing FAD, a b-type cytochrome, and Mo-pterin prosthetic groups in a ratio of 1:1:1 (Howard & Solomonson, 1982). The strong visible absorbance of the b-type cytochrome of NR has enabled the redox properties of this center to be studied in detail (Kay

† This work was supported by Grants 1 RO1 GM32696 from the National Institutes of Health and 84-CRCR-1-1404 from the United States Department of Agriculture.

[1] Abbreviations: NR, nitrate reductase; EPR, electron paramagnetic resonance; EDTA, ethylenediaminetetraacetic acid; CD, circular dichroism; CIP, corn inactivating protease; MV$^{\bullet+}$, methylviologen radical; FAD$^{\bullet-}$, flavin adenine dinucleotide semiquinone anion; FADH$^-$, flavin adenine dinucleotide hydroquinone.

0006-2960/88/0427-6142$01.50/0

et al., 1986). The midpoint potential of the heme has been shown to be pH dependent, suggesting the presence of a single ionizable group on the enzyme, with pK_{ox} = 5.8 and pK_{red} = 6.1. At pH 7.0 the midpoint potential (−164 mV) is similar to that of the enzyme isolated from the yeast *C. nitratophila* (−174 mV) (Notton et al., 1987) but substantially different from the values reported for the enzymes purified from spinach (Fido et al., 1979) and *A. braunii* (De la Rosa et al., 1980) of −60 and −73 mV, respectively. The functional significance of this difference is not yet understood.

In contrast to the heme, the visible spectral changes accompanying oxidation and reduction of the FAD and Mo–pterin centers[2] are comparatively weak and effectively obscured. Consequently, the electron affinity of the FAD bound to assimilatory nitrate reductase has not been previously determined. Current knowledge of the redox properties of Mo–pterin and FAD centers of NR derives from EPR studies of their paramagnetic redox states [Mo(V) and flavosemiquinone, $FAD^{\bullet-}$] at cryogenic temperatures (Jacob & Orme-Johnson, 1980; Gutteridge et al., 1983; Solomonson et al., 1984; Barber et al., 1987). The partially reduced forms of NR from *Chlorella* and spinach exhibit similar Mo(V) EPR spectra, the line shapes of which depend upon pH and the presence of anions such as phosphate and chloride (Gutteridge et al., 1983; Barber et al., 1987). The midpoint potentials for Mo(VI)/Mo(V) (−34 mV) and Mo(V)/Mo(IV) (−54 mV) have been measured by posing enzyme samples at room temperature in the presence of dye mediators and then freezing to 77 K followed by EPR analysis. As the midpoint potentials of both enzyme and mediators are inherently temperature dependent (Palmer & Olson, 1980) and pH changes can occur during freezing, it is possible that the electron distribution measured by this method may not accurately reflect that obtained at room temperature [e.g., Porras and Palmer (1982)].

We have found that all three centers contribute significantly to the CD spectrum of the enzyme in the region 300–650 nm and that the spectral changes due to each prosthetic group can be determined by using flavin and heme/Mo-containing fragments obtained by limited proteolysis of NR with a naturally occurring corn inactivator protease (CIP; Solomonson et al., 1984). This has enabled assignment of the observed CD bands to each chromophore. In this paper we have used CD spectral changes to monitor the redox states of FAD, heme, and Mo centers in order to determine midpoint potentials at room temperature. To confirm the Mo–pterin midpoint determinations, the values for the Mo(VI)/Mo(V) and Mo(V)/Mo(IV) couples were also determined by room temperature EPR titration of Mo(V).

Materials and Methods

Nitrate reductase was isolated from *C. vulgaris* by using the affinity purification procedure as described by Howard and Solomonson (1981) with the addition of a final chromatographic step involving preparative HPLC on a TSK4000 column. The enzyme exhibited an activity of greater than 80 units/mg of protein and an A_{413}/A_{280} ratio of higher than 1.8. The "large" (heme/Mo–pterin-containing) and "small" (FAD-containing) protein domains were prepared as described previously by using limited proteolysis with CIP followed by separation of the two fragments by chromatography on a Sephacryl S-300 column (Solomonson et al., 1984). Nitrate reductase heme- and FAD-containing domains were quantified by using extinction coefficients of 117 mM^{-1} cm^{-1} at 413 nm (Solomonson et al., 1984) and 11.3 mM^{-1} cm^{-1} at 460 nm (Ghisla, 1980), respectively.

Spectrophotometric Measurements. Optical spectra were recorded by a Shimadzu UV-260 spectrophotometer (Columbia, MD) equipped with a stirred, thermostated cuvette and interfaced to an Apple IIe microcomputer for spectra storage and manipulation. Circular dichroism spectra were recorded on a Jasco J-500C spectropolarimeter. Signal intensity was calibrated by using aqueous solutions of *d*-10-camphorsulfonic acid. Measurements in which the redox potential was not controlled were performed by using a sealed 1-cm path length cell of 100-μL volume. Spectra were digitized by using a Zenith 158PC fitted with a digitizing tablet (Summagraphics) and graphics plotter for base-line correction and the calculation of difference spectra.

Visible and CD Potentiometric Titrations. Visible and CD potentiometric titrations were performed at 25 °C in a volume of 1.25 mL in a 1-cm path length stirred cuvette equipped with a Ag/AgCl micro reference electrode (Microelectrodes, Inc.) and a gold wire indicating electrode, in a configuration similar to that described by Dutton (1978). The cuvette was sealed with a septum through which additions of reductant (20 mM reduced methylviologen, generated by H_2 reduction over a Pt catalyst) or oxidant [20 mM $K_3Fe_3(CN)_6$] were made. The sample was maintained under anaerobic conditions by a positive pressure of oxygen-free argon. The following redox mediators (10 μM each) were added to ensure complete redox equilibration: methylene blue (E_m' = +10 mV), 2,5-dihydroxybenzoquinone (E_m' = −60 mV), indigodisulfonic acid (E_m' = −125 mV), 2-hydroxy-1,4-naphthoquinone (E_m' = −137 mV), anthraquinone-2,7-disulfonate (E_m' = −182 mV), anthraquinone-2-sulfonate (E_m' = −225 mV), phenosafranine (E_m' = −255 mV), safranine T (E_m' = −289 mV), and neutral red (E_m' = −325 mV). Oxidation–reduction midpoint potentials, expressed relative to the standard hydrogen electrode, were obtained from the experimental data points by comparison with theoretical Nernst curves using a least-squares analysis.

Room Temperature EPR Potentiometric Titrations. Room temperature EPR potentiometric titrations were performed by using a Varian E109 Century Series spectrometer (Varian Associates, Palo Alto, CA) operating at 9 GHz with 100-kHz modulation and equipped with a TM102 wide-bore cavity. Mo(V) spectra were recorded by using a modulation amplitude of 0.32 mT and an incident microwave power of 50 mW from enzyme samples contained in a "high sensitivity" aqueous flat cell (0.1 × 17 × 55 mm) modified to include a Ag/AgCl micro reference electrode and a gold indicating electrode (Kay & Barber, 1987), maintained under anaerobic conditions by the passage of oxygen-free argon. Reductive and oxidative titrations were performed by addition of reduced methylviologen (20 mM) or $K_3Fe_3(CN)_6$ (20 mM), respectively. Following each addition of reductant or oxidant, the sample was gently mixed and allowed to equilibrate. Mixing and equilibration were continued until the indicated potentials before and after mixing were identical (typically 10 min), and then spectra were recorded. Titrations were typically performed by using a total volume of 1.25 mL containing NR (45 μM heme) in the presence of the same mixture of dye mediators (30 μM each) as used for the CD potentiometric titrations. Double integrations of the experimental Mo(V) spectra were performed as described by Wyard (1965) by using potassium nitrosodisulfonate (ICN Pharmaceuticals, Plainview, NY) as

[2] The term "Mo–pterin center" refers to the complex of Mo, molybdopterin, and associated protein ligands to Mo.

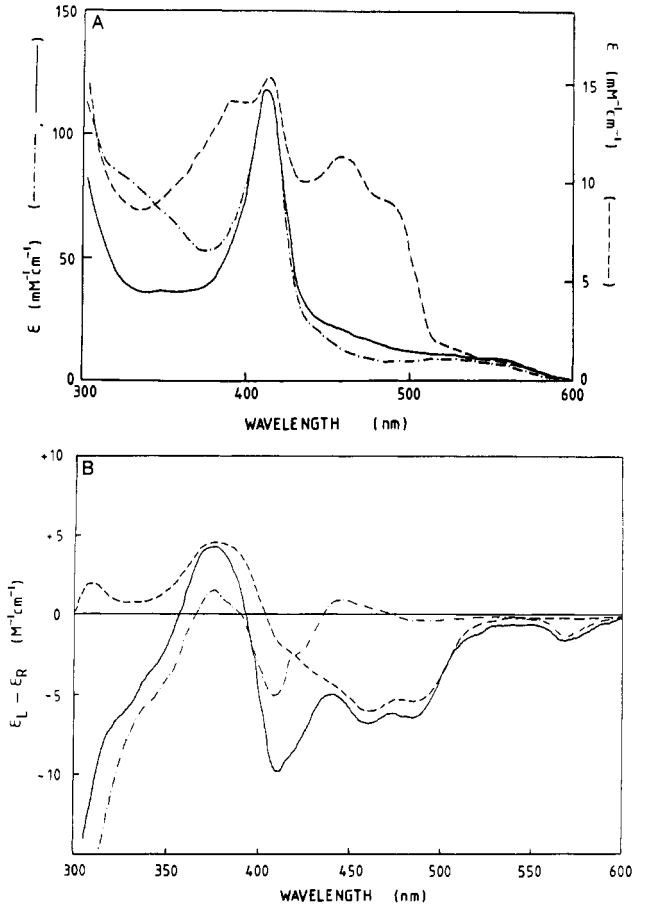

FIGURE 1: Visible and CD spectra of oxidized intact NR and fragments obtained by limited proteolysis. Spectra were recorded in 50 mM MOPS buffer, containing 0.1 mM EDTA, pH 7.0. (A) Visible spectra. (B) CD spectra. Intact enzyme (—, 7 μM heme), large domain (-·-, 8 μM heme), and small domain (---, 46 μM flavin).

standard (Palmer, 1967). EPR integrations were corrected to reflect the low molybdenum content of the enzyme (0.72 Mo/subunit), determined by colorimetric analysis (Solomonson et al., 1975). Oxidation–reduction potentials were calculated by fitting the experimental data points with the theoretical Nernst curve for the intermediate species formed by two consecutive one-electron reduction processes, using a least-squares procedure.

Results

Visible and CD Spectra. The visible spectrum of oxidized NR is shown in Figure 1A. The spectrum was dominated by the absorbance of the b-type cytochrome with maxima at 413 (Soret transition) and 550 nm (α band). No contributions due to either FAD or the Mo–pterin group could be resolved in this spectrum. A similar spectrum was obtained for the heme/Mo–pterin-containing large fragment obtained following limited proteolysis using CIP and chromatographic separation of the products. No Mo–pterin contributions to the visible spectrum could be resolved, consistent with previous reports of low absorption coefficients for the isolated Mo–pterin prosthetic group (Johnson et al., 1980), the Mo–pterin center of xanthine oxidase (Porras & Palmer, 1982), and the isolated Mo–pterin-containing protein domain of sulfite oxidase (Garner et al., 1982). In contrast, flavin absorbance bands were apparent at 460 and 487 nm in the FAD-containing small domain but were too weak to be clearly resolved in intact NR. Preparations of the FAD-containing small domain were found to contain traces of heme, detectable at 413 nm. The extent of contamination of the flavin domain with heme was calculated to be less than 7% from the absorbance change at 423 nm upon reduction by dithionite, using 416 nm as an isosbestic wavelength (Kay et al., 1986).

The corresponding CD spectra of oxidized native NR, large and small domains, are shown in Figure 1B. Optically active transitions giving rise to positive CD in the FAD-containing fragment were observed at 311 and 375 nm (positive CD) and 460 and 487 nm (negative CD). In addition, a weak negative shoulder was detected at 433 nm. Similar transitions could be discerned underlying the more complex spectrum of intact NR but were not found in the heme/Mo-containing large domain. The assignment of these features to FAD was confirmed during potentiometric titrations when changes in these features occurred at potentials commensurate with flavin reduction (see below) and are due to the interaction of the FAD isoalloxazine ring with the apoprotein, since unbound oxidized FAD is essentially planar (Dixon et al., 1979) and so has very weak optical activity at these wavelengths.

The large domain, containing both heme and Mo–pterin, showed negative CD at 415 nm with an inflection at 424 nm and negative CD at 570 nm, close to the heme Soret and α visible absorption bands, respectively. In addition, a weak shoulder was detected at 330 nm in the intense negative transition below 360 nm. The CD spectrum of native NR closely resembled that of the sum of the large and small domains (Figure 1B). Given the extreme sensitivity of CD to the immediate environment of chromophores, this suggested that proteolysis did not significantly disrupt prosthetic group binding to the apoprotein.

The corresponding reduced, visible, and CD spectra of native NR and the two fragments are shown in parts A and B of Figure 2, respectively. Reduction by dithionite shifted (to 423 nm) and intensified the visible heme Soret transition while intensifying the α (557 nm) and β bands (527 nm) in both native NR and the large domain, as previously reported (Solomonson et al., 1975) (Figure 2A). Reduction of the small domain resulted in a decrease in absorbance in the visible region, as occurs when free FAD is reduced. Consequently, the FAD optical activity and hence the CD bands were lost upon reduction with methylviologen (Figure 2B). The loss of the flavin CD transitions following reduction was also apparent in intact NR (Figure 2B). However, in the CD spectrum of reduced intact NR, the presence of a few percent of unreduced FAD was suggested by the minor differences between this spectrum and that of reduced large domain (Figure 2B). Reduction of the large domain and intact NR resulted in the appearance of CD couplets at the wavelengths of the Soret and α transitions. That these couplets were due to reduced cytochrome *b* was confirmed by potentiometry (see below). The shoulder in the CD spectrum of intact NR and large domain at 333 nm increased upon reduction. An increase in CD at this wavelength has previously been reported following reduction of the Mo–pterin domain from the related enzyme sulfite oxidase (Garner et al., 1982). These results suggested that all three prosthetic groups contributed to the observed CD spectrum of NR.

Potentiometric Titrations. Previous work has provided values for the midpoint potentials (pH 7.0, 25 °C) of the heme (Kay et al., 1986) and Mo–pterin (Solomonson et al., 1984) centers in *Chlorella* NR. The heme midpoint potential was found to be −164 mV (n = 1) by visible potentiometric titrations, while the midpoint potentials for the Mo(VI)/Mo(V) and Mo(V)/Mo(IV) couples were found to be −34 and −54 mV, respectively, by using low-temperature EPR potentiometric titrations.

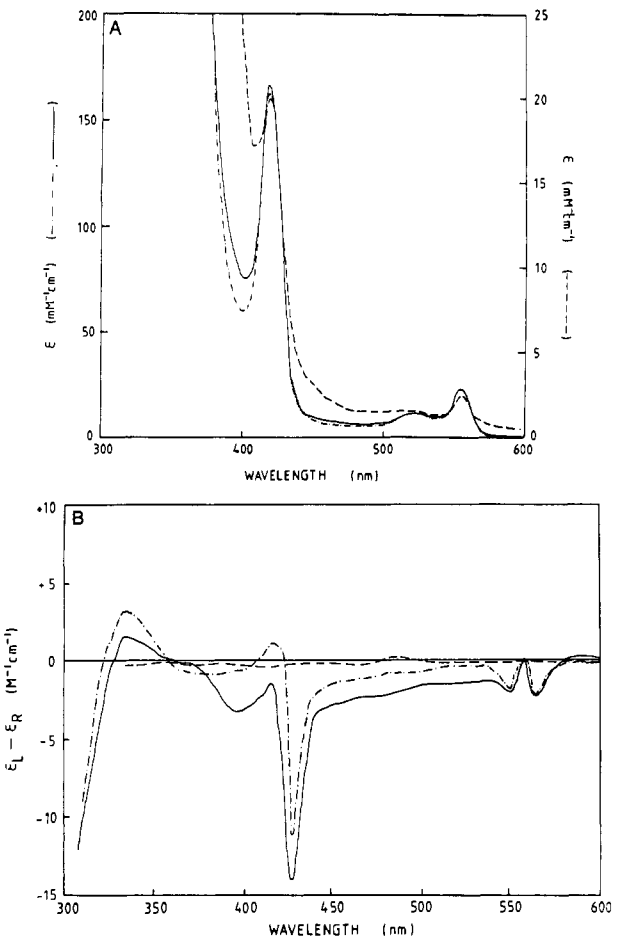

FIGURE 2: Visible and CD spectra of reduced intact NR and fragments obtained by limited proteolysis. (A) Visible spectra. (B) CD spectra. Spectra were recorded by using the same conditions given in Figure 1 except that reduced visible spectra were recorded following addition of dithionite solution, while samples for CD were reduced by using $MV^{\cdot+}$.

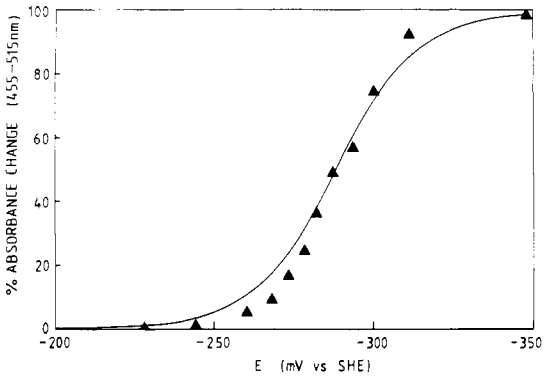

FIGURE 3: Visible potentiometric redox titration of the NR FAD-containing fragment. FAD-containing proteolytic domain (12 μM FAD) in 50 mM MOPs and 0.1 mM EDTA, pH 7.0, in the presence of redox mediators (0.5 μM anthraquinone-2,7-disulfonate, 0.5 μM anthaquinone-2-sulfonate, and 1 μM benzylviologen) was poised at the indicated redox potentials by using methylviologen (20 mM $MV^{\cdot+}$) as reductant. Flavin reduction was measured at 455 nm by using 515 nm as a reference, and the data are fitted to the theoretical Nernst curve (n = 2, E_m' = −286 mV).

To obtain a preliminary estimate of the midpoint potential of the FAD center ($FAD/FADH_2$), visible potentiometric titrations were performed by using the isolated flavin fragment. The results of a typical titration are shown in Figure 3. At pH 7, flavin reduction monitored at 450 nm corresponded to a single process with a midpoint potential of −286 mV (n = 2), suggesting the formation of very little semiquinone species.

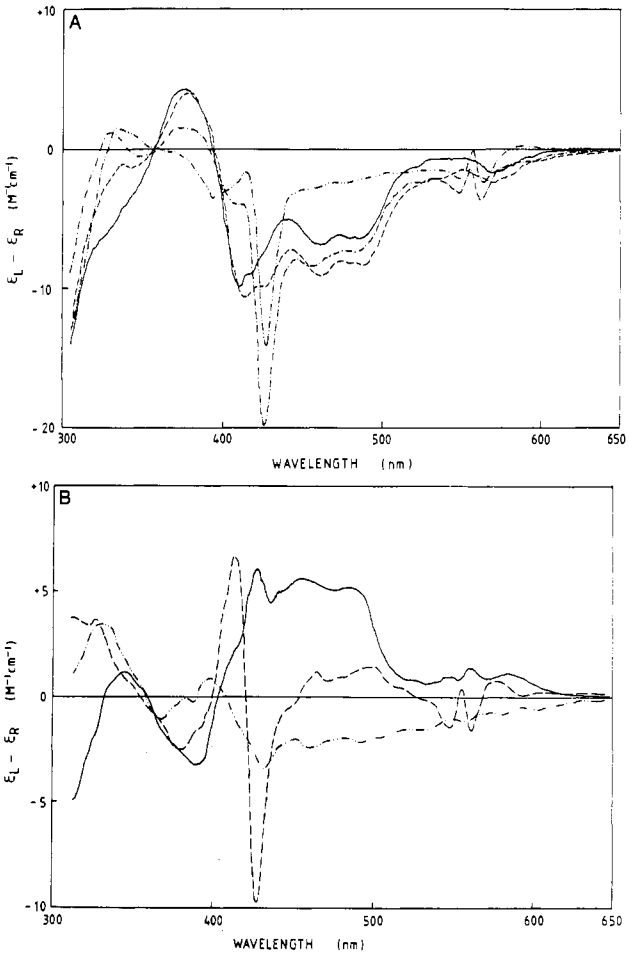

FIGURE 4: Controlled potential and CD difference spectra obtained for NR. (A) CD spectra of NR (10 μM heme) were recorded at controlled potentials by using $MV^{\cdot+}$ reduction in the presence of dye mediators (10 μM). The spectra correspond to the potentials +115 mV (—), −84 mV (- - -), −241 mV (-·-), and −341 mV (-··-). (B) CD difference spectra obtained for the reduced–oxidized forms of the three prosthetic groups: Mo–pterin (-··-); heme (- - -); flavin (—). The difference spectrum for Mo–pterin is predominantly Mo(IV) − Mo(VI). The percentage of Mo present as Mo(V) at a potential of −84 mV, calculated from the room temperature midpoint potentials in Table I, would be between 9 and 15%.

The wide separation of midpoint potentials for the three centers suggested it might be possible to poise NR at successive intermediate redox potentials so that the Mo–pterin center, heme, and flavin prosthetic groups would be successively reduced (Figure 4A), yielding the CD changes accompanying reduction of each individual chromophore. Optimum potentials were calculated by utilizing the midpoint potentials for the three centers given above such that each individual center would be maximally reduced while the remaining two were either maximally oxidized or maximally reduced according to the relation

$$E = E_{m1} - \frac{n_1(E_{m2} - E_{m1})}{n_1 + n_2}$$

where the subscripts 1 and 2 denote the midpoint potentials and n values of each successive redox couple. At the intermediate potentials selected, the percentage of each center in the undesired redox state would be expected to be less than 5%.

To ensure efficient redox equilibration, a selection of dye mediators were added to samples of NR. Control titrations showed that while the mediators did not contribute to the CD spectrum at the wavelengths used to examine NR (Porras &

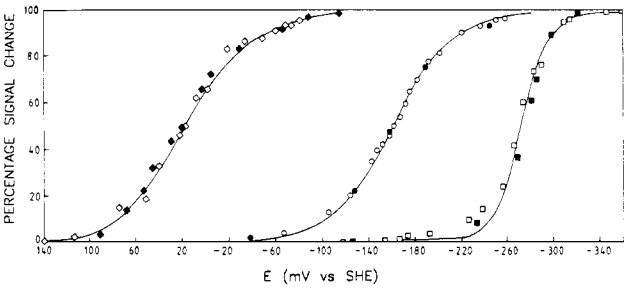

FIGURE 5: CD potentiometric titration of the Mo–pterin, heme, and flavin centers of NR at 25 °C. NR (20 μM heme) in 50 mM MOPS buffer, containing 0.1 mM EDTA, pH 7.0, was reduced or oxidized by additions of reduced methylviologen (20 mM) or $K_3Fe(CN)_6$ (20 mM) in the presence of dye mediators. The degree of reduction of the Mo–pterin center was followed at 333 nm, the heme at (423–416 nm), and FAD reduction at 460 nm: (◇) 333 nm; (○) 423–416 nm; (□) 460 nm. Closed and open symbols represent oxidative and reductive titrations, respectively.

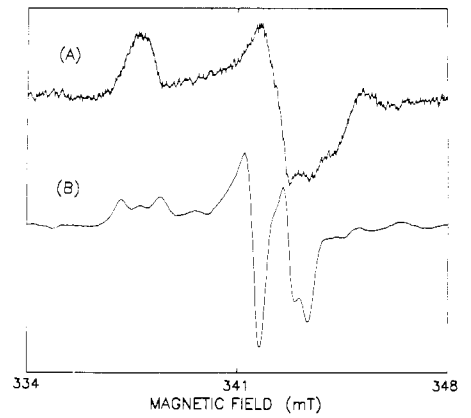

FIGURE 6: Comparison of Mo(V) EPR spectra obtained at room temperature and 173 K. EPR spectra were recorded at room temperature (A) and low temperature (B) for sample of enzyme (12 and 38 μM heme) poised at controlled potentials of +5 and −42 mV, respectively, in 50 mM MOPS buffer, containing 0.1 mM EDTA, pH 7.0. Spectra were recorded by using a microwave power of 5 mW and a modulation amplitude of 3.2 G. The field scale corresponds to a microwave frequency of 9.427 GHz.

Palmer, 1982), they absorbed sufficient light to decrease the observed spectral S/N ratio, precluding their use at concentrations above 10 μM each. Samples of NR were poised by using reduced methylviologen as reductant to within 5 mV of the values given in the legend to Figure 4. During the 20 min required to record each spectrum, a slow oxidative drift of potential (typically <1 mV/min) made it necessary to occasionally repoise the sample and record the spectrum as overlapping sections. Rescanning of the spectra indicated that this introduced minimal error, presumably because at these intermediate potentials the degree of reduction of the centers is least sensitive to small perturbations in potential.

Decreasing the redox potential from +125 to −84 mV, so that only the Mo–pterin center would be expected to become reduced, caused an increase in CD at 333 nm together with a broad decrease in CD in the wavelength range 400–600 nm (Figure 4A). Comparison of the CD difference spectrum for Mo–pterin and heme reduction (Soret region, Figure 4B) indicated that very little of these changes could be attributed to heme reduction. The CD changes for the Mo–pterin center of NR reported here are similar to those reported for the isolated Mo–pterin-containing domain of sulfite oxidase following reduction of the Mo center from Mo(VI) to Mo(IV) by sulfite (Garner et al., 1982). Decreasing the applied potential to −241 mV selectively reduced the heme (Figure 4A), causing the Soret and α negative CD bands to split into couplets with maxima at 413 and 557 nm and minima at 426 and 566 nm, respectively. Similar results were obtained by sequential reduction of the Mo–pterin and heme components of the large domain (results not shown). Decreasing the potential to −341 mV resulted in the apparent complete reduction of all the centers, since lower potentials had no further effect on the observed spectrum and the FAD CD features at 375, 460, and 487 nm were lost, as previously described for the reduction of the small domain. The similarity of the FAD environment in intact NR and the small domain was further indicated by comparison of the small-domain CD (Figure 1B) and the inverted difference spectrum for FAD reduction in intact NR (Figure 4B).

Potentiometric titrations of all three centers in both oxidative and reductive directions were performed by using the wavelengths given in the legend to Figure 5. Using the wavelengths corresponding to the heme Soret transition couplet maximum and minimum, fully reversible redox behavior corresponding to a midpoint potential of −162 mV and n = 1 was observed, in good agreement with a previous determination using visible spectroscopy (Kay et al., 1986). The reduction of FAD to flavin hydroquinone ($FADH^-$) was monitored by the disappearance of the negative CD bands of oxidized FAD at 460 and 489 nm. In both reductive and oxidative titrations, FAD exhibited a midpoint potential of −272 mV and an n value of 2 (Figure 5). In addition, the amplitude of the reoxidized FAD spectrum was often diminished following prolonged incubation of NR in the fully reduced state, suggesting partial dissociation of the reduced flavin from the enzyme. To examine the extent of $FAD^{\bullet-}$ formation, samples of NR were withdrawn anaerobically from the titration vessel, rapidly frozen in liquid nitrogen, and examined by EPR. Less than 1%[3] of the FAD was present in the semiquinone form, suggesting that the flavosemiquinone is extremely thermodynamically unstable in partially reduced NR in the absence of NAD(H). It has previously been shown that anionic flavosemiquinone is readily generated in NR when NADH, but not methylviologen or dithionite, is used as the reductant (Solomonson & Barber, 1984).

The increase in CD at 333 nm that was indicative of changes in the redox state of the Mo–pterin center was potentiometrically titrated as shown in Figure 5. The resulting curve was too broad to be consistent with a single n = 2 process corresponding to the concerted interconversion of Mo(VI) and Mo(IV) but instead appeared biphasic, consisting of an initial wave, centered at positive potential and corresponding to the major portion of the overall signal change followed by a second wave of significantly lower amplitude centered at negative potential. Least-squares analysis, assuming two consecutive one-electron redox processes contributing unequally to the observed signal change, gave a best fit corresponding to E_{m1}' = +26 mV and E_{m2}' = −40 mV with the E_{m1}' couple contributing 80% of the overall signal change. This theoretical line is shown fitted to the data points in Figure 5.

To confirm that the biphasic CD changes observed at 333 nm were due to successive reduction steps corresponding to the conversion of Mo(VI) to Mo(V) and Mo(IV), we utilized room temperature EPR potentiometry to directly monitor the appearance and disappearance of Mo(V) during the titration.

[3] We have estimated the concentration of $FAD^{\bullet-}$ as <1% by determining the minimum signal amplitude that could be detected in low-temperature EPR potentiometric titrations using optimum spectrometer settings and maximum gain, using the flavoprotein xanthine oxidase as a reference standard at equivalent flavin concentration.

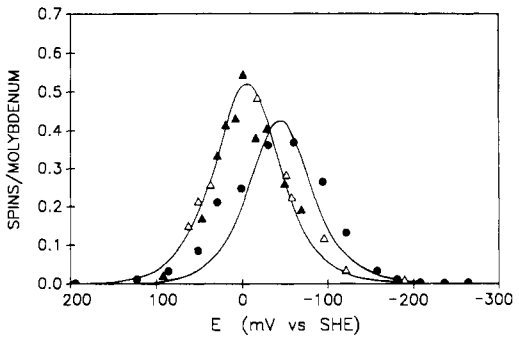

FIGURE 7: Behavior of the Mo(V) EPR signal during room temperature and low-temperature potentiometric EPR titrations. NR (12 and 38 μM heme) in 50 mM MOPS buffer, containing 0.1 mM EDTA, pH 7.0, was poised at controlled potentials in the presence of dye mediators (15 and 40 μM each mediator) by using either a modified EPR flat cell or standard titration vessel. In the former case, EPR spectra were recorded following attainment of equilibrium; for the latter case, samples were removed, frozen in liquid N_2, and then subsequently analyzed by EPR spectroscopy. Data points were obtained for both room temperature (△) and low-temperature (○) titrations. Theoretical Nernst curves fitted to the data points correspond to the potentials for the Mo(VI)/Mo(V) and Mo(V)/Mo(IV) redox couples of +15 and −25 mV for the room temperature titration and −34 and −54 mV for the low-temperature titration, respectively. Closed and open symbols represent titration in the reductive and oxidative directions, respectively.

Previous potentiometric titrations of NR have involved poising the enzyme at controlled potentials at 25 °C followed by freezing to 77 K for subsequent EPR analysis. Representative Mo(V) spectra obtained during potentiometric titrations in 50 mM MOPS buffer (pH 7.0) involving either room temperature or low-temperature (173 K) EPR analysis are shown in Figure 6. At room temperature, the Mo(V) signal was significantly broadened and exhibited near-axial symmetry with no clearly defined superhyperfine structure. However, at low temperature, the Mo(V) species was considerably sharper and showed superhyperfine splitting due to the presence of a single coupled proton.

The behavior of both the room temperature and low-temperature EPR signals during potentiometric titrations is shown in Figure 7. At room temperature and at potentials more positive than 120 mV, no Mo(V) signal was detectable. However, as the potential was decreased, the signal was observed to appear, reach a maximum amplitude at approximately −5 mV, and then decrease in intensity as the potential was further decreased. Similar behavior was observed when titration was performed in an oxidizing mode. Comparison of the room temperature behavior with that obtained for frozen samples showed two significant differences. At room temperature, the integrated intensity of the maximum signal corresponded to approximately 0.52 spin/Mo, in contrast to an integrated intensity for the frozen samples of 0.46 spin/Mo. In addition, the potential for maximum signal formation was shifted approximately 40 mV more positive than that for the frozen samples. Best-fit values for the midpoint potentials for the Mo(VI)/Mo(V) and Mo(V)/Mo(IV) couples obtained with room temperature EPR were found to be +15 and −25 mV, respectively, compared with the values of −34 and −54 mV, respectively, obtained following EPR analysis of frozen samples.

Discussion

The objective of this study was to characterize the CD spectral properties of the prosthetic groups of assimilatory nitrate reductase from *Chlorella* to facilitate measurement of the oxidation–reduction midpoint potentials of the flavin, heme, and Mo–pterin centers at room temperature. The strong absorbance of the heme group has previously precluded study of FAD and Mo–pterin in intact NR by visible spectroscopy. While valuable information concerning the nature of the flavin semiquinone and Mo(V) species of NR has been gained by using low-temperature EPR spectroscopy, midpoint potentials measured at cryogenic temperatures may differ significantly from those determined at room temperature (Porras & Palmer, 1982) since midpoint potentials are inherently temperature dependent.

Table I: Comparison of Oxidation–Reduction Midpoint Potentials for *Chlorella* Nitrate Reductase[a]

redox couple	visible spec	CD spec	room EPR	low EPR[b]	microcoulometry[c]
Mo(VI)/Mo(V)		+26	+15	−34	+16
Mo(V)/Mo(IV)		−40	−25	−54	−27
Mo(VI)/Mo(IV)		−7	−5	−44	−6
$heme_{ox/red}$	−164[d]	−162			−172
$FAD/FAD^{\cdot-}$		−372			
$FAD^{\cdot-}/FADH_2$		−172			
$FAD/FADH_2$	−286[e]	−272			−283

[a] All titrations were performed in 50 mM MOPS and 0.1 mM EDTA buffer (pH 7.0) in the presence of dye mediators. Microcoulometry, visible, CD, and room temperature EPR titrations were performed at 25 °C. For low-temperature EPR titrations, samples were poised at the desired potential at 25 °C and then frozen in liquid N_2 for EPR analysis. [b] Data from Solomonson et al. (1984). [c] Data from Spence et al. (1987). [d] Data from Kay et al. (1986). [e] Proteolytic small domain.

In the present study limited proteolysis of NR into FAD- and heme/Mo-containing fragments and selective reduction of the prosthetic groups have allowed features of the CD spectrum to be assigned to each redox center. The isoalloxazine ring of free FAD is planar in the oxidized state (Dixon et al., 1979) and Fe protoporphyrin IX is inherently symmetrical (C_{2v} or D_{2h}), preventing significant optical rotation by either chromophore at visible wavelengths when separated from the apoprotein (Schellman, 1969). The CD spectra are induced by the protein environment, which causes asymmetry in the environment of the chromophore, and the spectrum is also sensitive to the redox state of the center.

The FAD-containing small domain of NR includes the NADH-binding site and catalyzes NADH-linked ferricyanide reduction (Solomonson et al., 1986). Proteolytic cleavage of NR into FAD- and heme/Mo-containing domains did not appreciably alter the flavin CD, suggesting that the protein environment of FAD was unchanged. This view was supported by the similarity of the flavin midpoint potentials for intact NR and the FAD-containing proteolyzed domain (−272 and −286 mV, respectively, Table I). Also, the CD spectrum of intact NR was close to the sum of those of the large and small domains combined, indicating little perturbation of the environment of the heme or Mo–pterin centers by proteolysis. This is consistent with the observation that the heme midpoint potential was unaltered by limited proteolysis (Kay et al., 1986).

At least three optically active visible transitions occur in flavoproteins, centered roughly at 450, 375, and 310 nm (Song, 1969). The transition centered at 460 nm is a π–π^* transition (Weber, 1966; Edmondson & Tollin, 1971) that is partially resolved into three vibronic bands in many flavoproteins (Penzer & Radda, 1966). Increased resolution of these bands and a blue shift in peak wavelengths have been reported for flavin derivatives upon transfer from aqueous to nonpolar solvents (Harbury et al., 1959; Kotaki et al., 1967). The degree of resolution of CD bands observed in the present study and the comparatively pronounced band at 487 nm in the visible

spectrum suggest a hydrophobic rather than hydrophilic environment for this chromophore. The band at 375 nm is also a $\pi-\pi^*$ transition, with some $n-\pi^*$ character consistent with the large solvent-induced shifts reported (Eweg et al., 1980). The transition typically shows little resolution into vibronic components, as in this work. A transition at 311 nm is observed in some flavoproteins, but not others (Edmonson & Tollin, 1971; Scola-Nagelschneider et al., 1972), and has been suggested to be either a weak flavin transition not readily resolved by visible spectroscopy (Song, 1969) or alternatively a tryptophan residue that may interact with the flavin (Ananthanarayanan & Bigelow, 1969).

The loss of optical activity of FAD in both NR and the small domain upon reduction may be relevant to the redox properties of this center. In solution, oxidized isoalloxazine is planar but assumes the "butterfly" conformation when reduced, with approximately a 15° bend along the N_5-N_{10} axis (Fox et al., 1967; Dixon et al., 1979). Theoretical calculations suggest a barrier for the flattening of reduced flavin of some 10–17 kJ/mol (Dixon et al., 1979). Enforced flattening of the reduced form, by protein–FAD interaction, may enhance the reducing power of the flavin for one- and two-electron transfer (Tauscher et al., 1973). Distortion of reduced isoalloxazine could account for enhanced rates of reduced flavin dissociation from several flavoproteins (Dixon et al., 1979). Flavin dissociation, detected as a reduction in the amplitude of the FAD CD spectrum, was apparent following prolonged incubation of NR in the reduced state. In the present study the midpoint potential for reduction of FAD ($n = 2$) was determined to be −272 mV. This is approximately 50 mV more negative than unbound FAD ($E_m' = -220$ mV). This difference indicates that oxidized FAD is bound to NR apoprotein more tightly than the fully reduced hydroquinone by approximately 10 kJ/mol. Less than 1% of the FAD anionic semiquinone (Solomonson et al., 1984) could be detected by EPR analysis during potentiometric titration, suggesting that the two one-electron midpoint potentials for FAD reduction are widely separated and reversed, such that $E_m'(FAD/FAD^{\bullet-})$ is lower than $E_m'(FAD^{\bullet-}/FADH^-)$ by at least 200 mV. Interestingly, NR from *Chlorella* has been reported to follow a rapid-equilibrium random-order sequential kinetic mechanism (Howard & Solomonson, 1981). This mechanism implies that neither product (NAD^+ or nitrite) is released before nitrite formation has occurred. It is therefore feasible that fully reduced flavin and a vacant NAD(H) binding site never occur simultaneously, precluding enhanced flavin dissociation.

The visible and CD spectra of the Mo–pterin prosthetic group has been reported for the related molybdoenzyme sulfite oxidase, following limited proteolysis of native enzyme into separate heme and Mo–pterin-containing peptides (Johnson & Rajagopalan, 1977; Garner et al., 1982). In the oxidized state, weak visible absorbance bands were observed at approximately 360 and 480 nm, which were lost following reduction by sulfite (Johnson & Rajagopalan, 1977). The similarity of the spectrum to those of Fe-S proteins led Johnson and Rajagopalan (1977) to suggest that the absorbance bands were mainly due to coordination of Mo with sulfur-containing ligands. Evidence for two to three sulfur ligands of Mo has been obtained by EXAFS for both sulfite oxidase (Cramer et al., 1981) and NR from *Chlorella* (Cramer et al., 1984). Fragmentation and isolation of a Mo–pterin-containing peptide of NR that is free of heme has not yet been reported. The visible spectrum of the Mo–pterin is therefore unknown; however, the Mo–pterin contributions to the CD spectra for the two enzymes appear similar. Selective reduction of NR molybdenum was accompanied by a broad decrease in CD in the wavelength range 410–650 nm and a pronounced increase in CD at 333 nm (Figure 3). Reduction of the Mo–pterin domain of sulfite oxidase by sulfite or dithionite also caused a broad decrease in CD between 430 and 600 nm, and an increase in CD in the wavelength range 340–420 nm occurred upon reduction to Mo(V) by sulfite (Garner et al., 1982).

Further indications that the optical activity at 333 nm may be due to asymmetry of Mo-S coordination rather than from optical activity of the ligands themselves come from an EXAFS study showing low symmetry of the Mo–pterin center (Cramer et al., 1984) and from model Mo complexes, e.g., $MoO_2[(R)\text{-cysOMe}]_2$, which has both a visible absorbance band at 350 nm and a shoulder in the CD spectrum at 330 nm (Garner et al., 1982).

This work provides the first complete determination of the oxidation–reduction midpoint potentials for all the redox couples of NR at room temperature. A comparison of all the values obtained for *Chlorella* NR by using optical and EPR potentiometry and microcoulometry (Spence et al., 1987) is given in Table I. These results provide the first example of the use of CD potentiometry to determine the midpoint potentials of the Mo–pterin center in a Mo-containing hydroxylase enzyme (Bray, 1980). Comparison of the CD and room temperature EPR results shows that both methods yield equivalent midpoint potentials, within experimental error, and confirm our assignments of the two waves in the CD titrations as being due to the successive formation of Mo(V) and Mo(IV). In addition, the values obtained for the Mo couples are in good agreement with the results obtained by microcoulometry. In contrast, the values obtained from the CD and room temperature EPR titrations for the Mo(VI)/Mo(V) and Mo(V)/Mo(IV) couples are significantly different from the values obtained for the previously published potentiometric titrations involving low-temperature EPR analysis. For both couples, the values obtained by using low-temperature EPR were more negative, by approximately 30–50 mV. These shifts in potential can be due to the effects of temperature on redox potentials, changes in the pH of the medium between 25 °C and the frozen state, or a combination of both. While the previous low-temperature EPR titrations were performed in zwitterionic buffers, which have been shown to minimize pH changes upon freezing (Williams-Smith et al., 1977), results for xanthine oxidase have shown that Mo potentials are pH dependent, and thus small shifts in pH would be expected to perturb the observed redox potentials. However, the pH shifts in MOPS buffer are generally in the direction of lower values ($\Delta pH/°C = -0.011$), which would tend to shift Mo potentials to higher values upon freezing. Similarly, lower temperatures usually result in the shift of midpoint potentials to higher values. Comparison of the midpoint potentials obtained at low and room temperature for NR indicates that EPR analysis of frozen samples yields lower potentials than room temperature measurements. A similar conclusion has been obtained from redox studies of the Mo center in xanthine oxidase (Porras & Palmer, 1982).

The midpoint potentials obtained for the flavin center show this to be the most negative group in the enzyme, however, with a potential still more positive than that of the NAD^+/NADH couple, the physiological donor. In addition, the flavin center is more negative than the cytochrome. Thus, reducing equivalents are able to be effectively transferred from NADH to flavin, from reduced flavin to heme, and from reduced heme to Mo with final transfer to nitrate. Our results suggest that FAD acts as an obligatory two-electron acceptor, which then

presumably transfers reducing equivalents sequentially to heme for reduction of Mo(VI) to Mo(IV). Thus, these results indicate that electron transfer between prosthetic groups during enzyme turnover is thermodynamically highly favorable.

ACKNOWLEDGMENTS

We thank Dr. Ann Oaks of McMaster University, Ontario, for generously supplying the corn inactivator protease used in these studies.

REFERENCES

Ananthanarayanan, V. S., & Bigelow, C. C. (1969) *Biochemistry 8*, 3717–3723.

Barber, M. J., Notton, B. A., & Solomonson, L. P. (1987) *FEBS Lett. 213*, 372–374.

Bray, R. C. (1980) *Adv. Enzymol. Relat. Areas Mol. Biol. 51*, 107–165.

Cramer, S. P., Wahl, R., & Rajagopalan, K. V. (1981) *J. Am. Chem. Soc. 103*, 7721–7727.

Cramer, S. P., Solomonson, L. P., Adams, M. W. W., & Mortenson, L. E. (1984) *J. Am. Chem. Soc. 106*, 1467–1471.

De la Rosa, M. A., Diez, J., Vega, J. M., & Losada, M. (1980) *Eur. J. Biochem. 106*, 249–256.

Dixon, D. A., Lindner, D. L., Branchaud, B., & Lipscomb, W. N. (1979) *Biochemistry 18*, 5770–5775.

Dutton, P. L. (1978) *Methods Enzymol. 54*, 411–435.

Edmondson, D. E., & Tollin, G. (1971) *Biochemistry 10*, 113–123.

Eweg, J. D., Muller, F., van Dam, H., Terpstra, A., & Oskam, A. (1980) *J. Am. Chem. Soc. 102*, 51–61.

Fido, R. J., Hewitt, E. J., Notton, B. A., Jones, O. T. G., & Nasrulhaq-Boyce, A. (1979) *FEBS Lett. 99*, 180–182.

Fox, J. L., Laberge, S. P., Nishimoto, K., & Forster, L. S. (1967) *Biochim. Biophys. Acta 136*, 544–550.

Garner, C. D., Buchanan, I., Collison, D., Mabbs, F. E., Porter, T. G., & Wynn, C. H. (1982) *Proceedings of the Climax Fourth International Conference on the Chemistry and Uses of Molybdenum* (Barry, H. F., & Mitchell, P. C. H., Eds.) pp 163–168, Climax Molybdenum Co., Ann Arbor, MI.

Ghisla, S. (1980) *Methods Enzymol. 66*, 360–373.

Guerro, M. G., Vega, J. M., & Losada, M. (1981) *Annu. Rev. Plant Physiol. 32*, 169–214.

Gutteridge, S., Bray, R. C., Notton, B. A., Fido, R. J., & Hewitt, E. J. (1983) *Biochem. J. 213*, 137–142.

Harbury, H. A., LaNove, K. F., Loach, P. A., & Amick, R. M. (1959) *Proc. Natl. Acad. Sci. U.S.A. 45*, 1708–1717.

Howard, W. D., & Solomonson, L. P. (1981) *J. Biol. Chem. 256*, 12725–12730.

Howard, W. D., & Solomonson, L. P. (1982) *J. Biol. Chem. 257*, 10243–10250.

Jacob, G. S., & Orme-Johnson, W. H. (1980) in *Molybdenum and Molybdenum-Containing Enzymes* (Coughlan, M. P., Ed.) pp 327–344, Pergamon, New York.

Johnson, J. L., & Rajagopalan, K. V. (1977) *J. Biol. Chem. 252*, 2017–2025.

Johnson, J. L., Hainline, B. E., & Rajagopalan, K. V. (1980) *J. Biol. Chem. 255*, 1783–1786.

Kay, C. J., Solomonson, L. P., & Barber, M. J. (1986) *J. Biol. Chem. 261*, 5799–5802.

Kotaki, A., Naoi, M., Okuda, J., & Yagi, K. (1967) *J. Biochem. (Tokyo) 61*, 404–406.

Notton, B. A., Kay, C. J., Barber, M. J., Solomonson, L. P., Kau, D., Cannons, A. C., & Hipkin, C. R. (1987) *Fed. Proc., Fed. Am. Soc. Exp. Biol. 46*, A1007.

Palmer, G. (1967) *Methods Enzymol. 10*, 594–609.

Palmer, G., & Olson, J. S. (1980) in *Molybdenum and Molybdenum-Containing Enzymes* (Coughlan, M. P., Ed.) pp 187–220, Pergamon, New York.

Penzer, G. R., & Radda, G. K. (1966) *Q. Rev., Chem. Soc. 21*, 43–67.

Porras, A. G., & Palmer, G. (1982) *J. Biol. Chem. 257*, 11617–11626.

Schellman, J. A. (1969) *Acc. Chem. Res. 1*, 144–151.

Scola-Nagelschneider, G., & Hemmerich, P. (1972) *Z. Naturforsch., B: Anorg. Chem., Org. Chem., Biochem., Biophys., Biol. 27B*, 1044–1046.

Solomonson, L. P., & Barber, M. J. (1984) in *Flavins and Flavoproteins* (Bray, R. C., Engel, P., & Mayhew, S. G., Eds.) pp 247–250, de Gruyter, Berlin.

Solomonson, L. P., Lorimer, G. H., Hall, R. L., Borschers, R., & Leggett-Bailey, J. (1975) *J. Biol. Chem. 250*, 4120–4127.

Solomonson, L. P., Howard, W. D., Yamaya, T., & Oaks, A. (1984) *Arch. Biochem. Biophys. 233*, 469–474.

Solomonson, L. P., Barber, M. J., Howard, W. D., Johnson, J. L., & Rajagopalan, K. V. (1984) *J. Biol. Chem. 259*, 849–853.

Solomonson, L. P., Barber, M. J., Robbins, A. P., & Oaks, A. (1986) *J. Biol. Chem. 261*, 11290–11294.

Song, P. S. (1969) *Int. J. Quantum Chem. Symp. 3*, 303–316.

Spence, J., Barber, M. J., & Solomonson, L. P. *Biochem. J.* (submitted).

Sturtevant, J. M., & Tsong, T. Y. (1969) *J. Biol. Chem. 244*, 4942–4950.

Tauscher, L., Ghisla, S., & Hemmerich, P. (1973) *Helv. Chim. Acta 56*, 630–644.

Weber, G. (1966) in *Flavins and Flavoproteins* (Slater, E. C., & Veeger, C., Eds.) Elsevier, Amsterdam.

Williams-Smith, D. L., Bray, R. C., Barber, M. J., Tsopanakis, A. S., & Vincent, S. P. (1977) *Biochem. J. 167*, 593–600.

Wyard, S. J. (1965) *J. Sci. Instrum. 42*, 768–769.